Contribution from the Department of Chemistry,
University of Calgary, Calgary, Alberta, Canada T2N 1N4

Coordination Geometries and Relative Donor-Acceptor Abilities of CX and X_2 (X = O, S, Se, Te) and CX_2 and H_2CX (X = O, S) Complexed to $Ru(CO)_4$. Theoretical Study by the Hartree-Fock-Slater Transition-State Method

Tom Ziegler

Received December 26, 1985

The geometries and binding energies of CX and X_2 (X = O, S, Se, Te) and H_2CX and CX_2 (X = O, S) complexed to $Ru(CO)_4$ have been calculated by using the Hartree-Fock-Slater method. The calculated bond energies (kJ mol^{-1}) were as follows: D(Ru-CX) = 180 (CO), 237 (CS), 249 (CSe), 261 (CTe); D(Ru-X_2) = 133 (O_2), 244 (S_2), 246 (Se_2), 240 (Te_2); D(Ru-H_2CX) = 181 (H_2CO), 228 (H_2CS); D(Ru-CX_2) = 102 (CO_2), 157 (CS_2). The donor and acceptor abilities for CX increase along the series X = O, S, Se, and Te, and this trend is explained in terms of the drop in electronegativity from oxygen to tellurium. The calculated C-X force constants for complexed CX (mdyn $Å^{-1}$), k(C-X) = 16.4 (CO), 8.2 (CS), 6.1 (CSe), and 4.4 (CTe), are very similar to those calculated for free CX, k(C-X) = 18.6 (CO), 8.4 (CS), 6.2 (CSe), and 4.4 (CTe), except for CO. A possible explanation is given for why only k(CO) of complexed CO is reduced, although the back-donation to this ligand is smaller than that to CS, CSe, and CTe in $Ru(CO)_4CX$. The optimized X-X distances for X_2 in $Ru(CO)_4X_2$ were (Å) R(X-X) = 1.29 (O_2), 2.08 (S_2) 2.34 (Se_2), and 2.78 (Te_2). The distances in $Ru(CO)_4X_2$ are 0.2 Å longer than in free X_2 and are similar to those of X_2^-. Complexed H_2CX in the η^2 conformation have the hydrogens bent back by 30° and the C-X bond elongated by 0.1 Å according to the HFS calculations. The CX_2 ligands (X = O, S) are found to prefer the η^2-CX functionality rather than coordination through carbon by 145 (X = O) and 126 kJ mol^{-1} (X = S), respectively. A discussion is also given of the molecular and electronic structures of the $Ru(CO)_4$ fragment used in this investigation, as well as its saturated parent molecule $Ru(CO)_5$.

I. Introduction

The oxo ligands CO,[1] O_2,[2] CO_2,[3] and H_2CO[4] have a rather versatile coordination chemistry, with a number of different bonding modes to metal centers for each individual ligand, in which CO, CO_2, O_2, and H_2CO serve as donors as well as acceptors. The coordination chemistry of the corresponding thio, seleno, and telluro ligands CX,[5] X_2,[6] CX_2,[7] and H_2CX[8] (X = S, Se, Te), many of which are difficult to isolate in the free state, seems to be even richer, with metal complexes isostructural to those of the oxo ligands as well as metal complexes with bonding modes not realized by the oxo analogues.

The ability of CX, X_2, CX_2, and H_2CX to act as donors and acceptors, as well as their reactivity in the complexed state, seems to vary considerably along the seriers X = O, S, Se, and Te. Thus, CS and CSe appear[5] to be better σ-donors and π-acceptors than CO and can[9] in contrast to carbon monoxide insert into metal-hydride bonds by an intramolecular migratory insertion reaction. η^2-disulfur and -diselenium complexes are, in contrast to η^2 complexes of O_2, subject to electrophilic attacks,[10] and carbon disulfide is more readily complexed[7] than carbon dioxide.

We shall in the present study focus our attention on how the donor and acceptor abilities of η^1-CX and η^2-X_2, -H_2CX, and -CX_2 vary with the electronegativity of the chalcogen atoms, through the series X = O, S, Se, and Te. In order to make the comparisons on an equal footing we have considered all ligands as complexed to the same metal fragment ML_n, which in the following will be represented by $Ru(CO)_4$. All the calculations presented here were based on the LCAO-HFS method due to Baerends et al.[12] This method has already been applied in calculations on several transition-metal systems,[12] including a recent theoretical study[13] on the migratory aptitude of H and CH_3 toward CO and CS.

The method has, in conjunction with the generalized transition-state method,[14] the distinct advantage of providing a breakdown of the calculated bond energies into steric factors as well as contributions due to σ/π-donation and π^*-back-donation. Such a decomposition enables us to assess the relative donor and acceptor strength of different ligands as a function of X = O, S, Se, and Te.

II. Computational Details

The calculations reported in this work were carried out by utilizing the HFS-LCAO program system developed by Baerends et al.[11] The 4s, 4p, 4d, 5s, and 5p shells on Ru were represented by an uncontracted triple-ζ STO basis set.[15] The ns and np shells on C, O, P, S, Se, and Te were represented by a double-ζ STO basis set[15] augmented by a single STO d-orbital (ζ^C_{3d} = 2.5; ζ^O_{3d} = 2.0; ζ^P_{3d} = 1.4; ζ^S_{3d} = 1.8; ζ^{Te}_{5d} = 1.93), whereas 1s of H was represented by a double-ζ STO basis set[15] augmented by a single 2p STO (ζ^H_{2p} = 1.0). The electrons in shells of lower energy on C, O, P, S, Se, Te, and Ru were considered as core electrons and were treated by the frozen-core approximation according to the procedure due to Baerends et al.[11] A set of auxiliary s, p, d, f, and g STO functions[16] centered on all nuclei were used in order to fit the molecular density and represent the Coulomb and exchange potentials accurately in each SCF cycle.[11] The exchange scale factor α_{ex} was given the standard value[11] of α_{ex} = 70.

III. Electronc and Molecular Structures of $Ru(CO)_5$ and $Ru(CO)_4$. Initial Considerations

The main objective of the present study has been to assess the relative importance of donation and back-donation in the coor-

(1) Braterman, P. S. *Struct. Bonding (Berlin)* **1974**, *26*, 1.
(2) Lever, A. B. P.; Gray, H. B. *Acc. Chem. Res.* **1978**, *11*, 348.
(3) Darensbourg, D. J.; Kudaroski, R. A. *Adv. Organomet. Chem.* **1983**, *22*, 129.
(4) (a) Gambarotta, S.; Floriani, C.; Chiesi-Villa, A.; Guastini, C. *J. Am. Chem. Soc.* **1985**, *107*, 2985. (b) Gambarotta, S.; Floriani, C.; Chiesi-Villa, A.; Guastini, C. *J. Am. Chem. Soc.* **1982**, *104*, 2019. (c) Brown, K. L.; Clark, G. R.; Headford, C. E. L.; Mardesn, K.; Roper, W. R. *J. Am. Chem. Soc.* **1979**, *101*, 503.
(5) (a) Butler, I. M. *Acc. Chem. Res.* **1977**, *10*, 359. (b) Yaneff, P. V. *Coord. Chem. Rev.* **1977**, *23*, 183.
(6) Müller, A.; Jaegermann, W.; Enemark, J. H. *Coord. Chem. Rev.* **1982**, *46*, 245.
(7) Ibers, J. A. *Chem. Soc. Rev.* **1982**, *11*, 57.
(8) (a) Headford, C. E. L.; Roper, W. R. *J. Organomet. Chem.* **1983**, *244*, C53. (b) McCormick, F. B. *Organometallics* **1984**, *3*, 1924.
(9) Collins, T.; Roper, W. R. *J. Organomet. Chem.* **1978**, *73*, 159.
(10) Farrar, D. H.; Grundy, K. R.; Payne, N. C.; Roper, W. R.; Walker, A. *J. Am. Chem. Soc.* **1979**, *101*, 6577.
(11) Baerends, E. J.; Ellis, D. E.; Ros, P. *Chem. Phys.* **1973**, *2*, 41.
(12) (a) DeKock, R. L.; Baerends, E. J.; Boerrigter, P. M.; Hengelmolen, R. *J. Am. Chem. Soc.* **1984**, *106*, 3387. (b) Ziegler, T. *J. Am. Chem. Soc.* **1985**, *107*, 4453 and references therein.
(13) Ziegler, T.; Versluis, L.; Tschinke, V. *J. Am. Chem. Soc.* **1986**, *108*, 612.
(14) Ziegler, T.; Rauk, A. *Theor. Chim. Acta.* **1977**, *46*, 1.
(15) (a) Vernooijs, P.; Snijders, J. G.; Baerends, E. J. "Slater type basis functions for the whole periodic system", internal report; The Free University of Amsterdam: Amsterdam, The Netherlands, 1981. (b) Snijders, G. J.; Baerends, E. J. Vernooijs, P. *At. Data Nucl. Data Tables* **1982**, *26*, 483.
(16) Krijn, J.; Baerends, E. J. "Fit functions in the HFS-method"; internal report (in Dutch), The Free University of Amsterdam: Amsterdam The Netherlands, 1984.

0020-1669/86/1325-2721$01.50/0

dinative bonds between CO, O_2, CO_2, or H_2CO and a metal center and the change in donor–acceptor abilities as the oxo lignds are replaced by their thio, seleno, and telluro analogues, as well as the extent to which the various ligands are deformed on coordination.

It is in order to meet these objectives, and carry out the comparisons on an equal footing, most convenient to consider Y = CX, X_2, CX_2, and H_2CX (X = O, S, Se, Te) as complexed to the same metal fragment ML_n. A homologous series of YML_n complexes with a common ML_n fragment is, however, not known experimentally, and we have been forced to consider model systems. We have chosen $Ru(CO)_4$ as our model fragment, since most of the ligands considered here are known to complex to group 8D (group 8[34]) metals with at least one carbon monoxide group as a coligand. We shall now, as a convenient starting point, turn to a brief discussion of the molecular and electronic structure of $Ru(CO)_4$ as well as its coordinatively saturated parent molecule $Ru(CO)_5$.

The molecular structure of $Ru(CO)_5$ has not been determined by diffraction methods, but its IR spectrum[17] is consistent with a trigonal-pyramidal conformation **1** of D_{3h} symmetry. We find

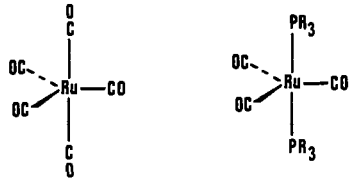

1 **2**

the d^8-pentacarbonyl $Ru(CO)_5$ in conformation **1** to have a low-spin electronic ground state with a vacant d_{z^2} orbital on the metal pointing along the 3-fold axis, and calculate the axial and equatorial Ru–CO bonds to be similar in length, with R_{eq}(Ru–CO) = 1.958 Å and R_{ax}(Ru–CO) = 1.945 Å. The similarity between R_{ax}(Ru–CO) and R_{eq}(Ru–CO) can be explained in terms of a competition between σ-bonding interactions, which are strongest in the axial positions, and π-bonding interactions, which are strongest[18] in the equatorial positions. In fact, the two d^8-pentacarbonyls $Mn(CO)_5^-$ and $Fe(CO)_5$,[19] for which X-ray or electron diffraction studies are available, have both similar axial and equatorial M–CO bond distances with the axial bond 0.01 Å longer in $Mn(CO)_5^-$ and 0.02 Å shorter in $Fe(CO)_5$. In our calculations on $Fe(CO)_5$ of conformation **1** we find R_{ax}(Fe–CO) = 1.77 Å and R_{eq}(Fe–CO) = 1.79 Å, compared to the experimental values of R_{ax}(Fe–CO) = 1.81 Å and R_{eq}(Fe–CO) = 1.83 Å.

The ruthenium carbonyls for which X-ray diffraction studies are available have phosphines in the axial positions, **2**, and equatorial R(Ru-CO) distances somewhat shorter than those calculated for $Ru(CO)_5$. Thus, $Ru(CO)_3(PCH_3)_2$[20] is observed to have R_{eq}(Ru–CO) = 1.90 Å, compared to R_{eq}(Ru–CO) = 1.96 Å calculated for $Ru(CO)_5$. It is, however, not surprising that R_{eq}(Ru–CO) is shorter for $Ru(CO)_3(PR_3)_2$ of conformation **2** than for $Ru(CO)_5$ of conformation **1**, since PR_3 relative to carbon monoxide is a stronger σ-donr and a weaker π-acceptor and is thus on both accounts able to enhance the back-donation to the π^* orbitals of the equatorial CO ligands, in comparison to two axial CO groups. We found in fact from our calculations that the substitution of two axial CO groups in **1** with two PH_3 ligands will reduce R_{eq}(Ru–CO) from 1.96 to 1.92 Å. For the analogous iron systems one observes clearly a shortening of R_{eq}(Fe–CO) in the phosphine-substituted complexes **2** compared to that in $Fe(CO)_5$. Thus, R_{eq}(Fe–CO) = 1.76 Å for $Fe(CO)_3(P(OCH_3)_3)_2$,[21]

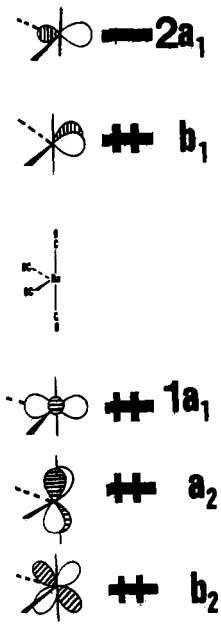

Figure 1. Orbital levels with schematic representation of the corresponding orbitals with the d^8 fragment $Ru(CO)_4$ of conformation **6**.

compared to R_{eq}(Fe–CO) = 1.83 Å for $Fe(CO)_5$, and we calculate R_{eq}(Fe–CO) = 1.74 Å for $Fe(CO)_3(PH_3)_2$ of conformation **2** and R_{eq}(Fe–CO) = 1.79 Å for $Fe(CO)_5$ of conformation **1**.

The coordinately unsaturated 16-electron species $Ru(CO)_4$ has been observed[22] as an intermediate in substitution reactions involving $Ru(CO)_5$, but its structure is not known. We calculate $Ru(CO)_4$ to have a low-spin (singlet) electronic ground state with a D_{2d} structure (**3**) where ϕ = 154°. The first electronically excited

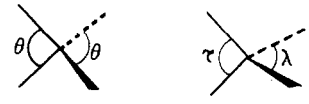

3 **4**

state, a triplet, in which $Ru(CO)_4$ has a C_{2v} structure (**4**) with λ = 114° and τ = 152° is however only 112 kJ mol^{-1} higher in energy. One might have expected $Ru(CO)_4$ in the singlet state to be square planar in analogy with most low-spin d^8 ML_4 complexes. Elian and Hoffmann[23] have, however, shown that the square-planar geometry for d^8 ML_4 systems is unstable with respect to a D_{2d} deformation if L is a strong π-acceptor such as CO, since the d_{z^2} orbital perpendicular to the ML_4 coordination plane is considerably stabilized in the course of a D_{2d} deformation by interacting with the π^*-acceptor orbitals on CO. This stabilziation according to our calculations amounts to 21 kJ mol^{-1} for $Ru(CO)_4$. It should be noted for the singlet state, that a distortion from **3** to the C_{2v} conformation **4** where τ = 120° and λ = 154° only requires 9 kJ mol^{-1}.

The corresponding $Fe(CO)_4$ system has been shown[24] to have a triplet ground state with a C_{2v} structure (τ = 120°, λ = 145°). It is, however, not uncommon that the 3d member, here $Fe(CO)_4$, in a homologous series of d^8 complexes is triplet (high spin) whereas the 4d and 5d members are singlets (low spin). This trend, which is observed in the series MCl_4^{2-} (M = Ni, Pd, Pt) and $M(PR_3)_4^+$ (M = Co, Rh, Ir), can readily be explained in terms of an increase in the energy gap between nonbonding and antibonding d-type orbitals of ML_4 as the overlaps between ligand-based orbitals and metal-based d-orbitals increase with increasing radial extent of the d orbitals down a triad. The spin polarization energy, which depends on two-electron-exchange integrals involving the nd-metal orbitals, will in addition in a triad be largest for the 3d element, which has the more contracted d orbitals, and

(17) Calderazzo, F.; Eplattenier, L. *Inorg. Chem.* **1967**, *6*, 1220.
(18) Rossi, A. R.; Hoffmann, R. *Inorg. Chem.* **1975**, *14*, 365.
(19) (a) Frenz, F. A.; Ibers, J. A. *Inorg. Chem.* **1972**, *11*, 1109. (b) Beagley, B.; Schmidling, D. G. *J. Mol. Struct.* **1974**, *22*, 466.
(20) Jones, R. A.; Wilkinson, G.; Galas, N. R. Hursthouse, M. B.; Malik, K. M. A. *Chem. Soc. Dalton Trans.* **1980**, 1771.
(21) Ginderow, P. D. *Acta Crystallogr., Sect. B: Struct. Crystallogr. Cryst. Chem.* **1974**, *B30*, 2798.
(22) Levison, J. J.; Robinson, S. D. *J. Chem. Soc. A* **1970**, 639.
(23) Elian, M.; Hoffmann, R. *Inorg. Chem.* **1975**, *14*, 1058.
(24) Poliakoff, M.; Turner, J. J. *J. Chem. Soc., Dalton Trans.* **1974**, *70*, 93.

Table I. Optimized R(Ru–CX) and R(C–X) Bond Distances (Å), Calculated k(Ru–CX) and k(C–X) Force Constants (mdyn Å^{-1}), and Calculated D(Ru–CX) Bond Energies (kJ mol^{-1}) in $Ru(CO)_4CX$ (X = O, S, Se, Te)

CX	R(Ru–CX)	R(C–X)	k(Ru–CX)	k(C–X)	D(Ru–CX)
CO	1.958	1.15 (1.14)[a]	2.47	16.4 (18.6)[b]	180
CS	1.891	1.56 (1.55)	2.78	8.2 (8.4)	237
CSe	1.886	1.70 (1.70)	3.10	6.1 (6.2)	249
CTe	1.885	1.94 (1.93)	3.15	4.4 (4.8)	261

[a] Calculated R(C–X) equilibrium distances for free CX. The corresponding experimental values for R(C–X) in free CX are R(CO) = 1.13 Å, R(CS) = 1.53 Å, and R(CSe) = 1.68 Å, according to ref 27. [b] Calculated k(C–X) force constants for free CX. The corresponding experimental values are k(CO) = 18.6, k(CS) = 8.47, and k(CSe) = 6.44, according to ref 27.

this will further favor the high-spin configuration for complexes of 3d elements in comparison to the 4d and 5d homologues.

We shall, in the following sections, primarily consider $Ru(CO)_4Y$ in conformation **5** where Y has replaced one of the equatorial CO ligands. The $Ru(CO)_4$ fragment will thus in $Ru(CO)_4Y$ adopt the butterfly structure **6** of C_{2v} symmetry, which we calculate to

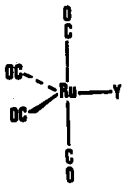

5

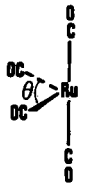

6

be between 117 (θ = 90°) and 16 kJ mol^{-1} (θ = 120°) higher in energy than conformation **3**. The $Ru(CO)_4$ fragment of geometry **6** has a low-spin electronic ground state as indicated in Figure 1, where we have sketched its well-known upper occupied and lower unoccupied orbitals. We shall now, in the next sections, turn to a discussion of how the $2a_1$ acceptor orbital (see Figure 1), as well as the b_2 and b_1 donor orbitals, interacts with the orbitals of Y.

IV. Donor and Acceptor Abilities of CO, CS, CSe, and CTe in $Ru(CO)_4CX$ (X = O, S, Se, Te)

Thiocarbonyl, and to a lesser extent selenocarbonyl, have previously been compared both theoretically[25] and experimentally[26] to CO as σ-donors and π-acceptors coordinated to a metal center. However, we present here the first study on the full series of chalcocarbonyls CX (X = O, S, Se, Te) complexed to the same fragment, $Ru(CO)_4$. Previous theoretical studies[25] on thiocarbonyl or selenocarbonyl complexes have concentrated on the qualitative aspects of the M–CX bonding modes. We present here in Table I calculated R(Ru–CX) and R(C–X) equilibrium bond distances and k(Ru–CX) and k(Ru–X) force constants, corresponding to $Ru(CO)_4CX$ of conformation **7** with CX in the equatorial position.

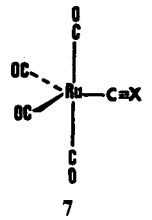

7

The equilibrium distances and force constants are further compared to R(C–X) and k(C–X) calculated for free CX, Table I.

It follows from Table I that D(Ru–CX) increases along the series X = O, S, Se, and Te with the steepest increment between CO and CS. Associated with the trend in D(Ru–CX) is a shortening of the Ru–CX bond distance and an increase in the Ru–CX force constant, again with the most pronounced change taking place between CX = CO and CX = CS; see Table I.

Table II. Decomposition of Calculated Bonding Energies D(Ru–CX) (kJ mol^{-1}) in $Ru(CO)_4CX$

CX	ΔE_{prep}	$\Delta E°$	ΔE_{A_1}	ΔE_{B_1}	ΔE_{B_2}	ΔE_{BD}	D(Ru–CX)[b]
CO	−16	−199	220	114	61	175[a]	180[c]
CS	−16	−204	241	142	74	216	237
CSe	−16	−209	242	153	79	232	249
CTe	−16	−224	250	169	82	251	261

[a] $\Delta E_{BD} = \Delta E_{B_1} + \Delta E_{B_2}$. [b] D(Ru–CX) = $\Delta E_{prep} + \Delta E° + \Delta E_{A_1} + \Delta E_{BD}$. [c] The contribution to D(Ru–CX) from ΔE_{A_2} is less than 1 kJ mol^{-1}.

The bonding between CX and $Ru(CO)_4$ can be described in terms of well-known concepts as a donation of charge from σ_{CX} to $2a_1$ of $Ru(CO)_4$ (**8a**) and a back-donation of charge from b_1

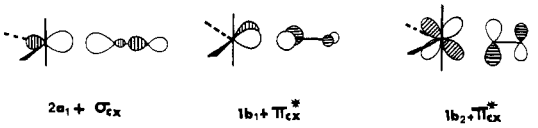

8a **8b** **8c**

or b_2 of $Ru(CO)_4$ to the two π^*_{CX} orbitals (**8b,c**). We have, in order to pinpoint the degree to which donation and back-donation are responsible for the calculated trends in Table I, decomposed the dissociation energy D(Ru–CX) into

$$D(\text{Ru–CX}) = \Delta E_{prep} + \Delta E° + \Delta E_{A_1} + \Delta E_{A_2} + \Delta E_{B_1} + \Delta E_{B_2} \quad (1)$$

The first term in eq 1, ΔE_{prep}, corresponds to the deformation of $Ru(CO)_4$ from **3** to **6**, whereas the second term, $\Delta E°$, corresponds to combining CX and $Ru(CO)_4$ of conformation **6** at the positions they have in $Ru(CO)_4CX$ (**7**), without allowing the electron density to relax. The term $\Delta E°$ is referred to as the steric interaction energy, as it represents the hard interaction between the two fragments. The last four terms in eq 1 represent the changes in density of the occupied orbitals with a_1, a_2, b_1, and b_2 symmetries, respectively, as the electron distribution is allowed to relax to the final density of $Ru(CO)_4CX$. The term ΔE_{A_1} can thus be related to the donation from σ_{CX} to $2a_1$ of $Ru(CO)_4$ (**8a**), and ΔE_{B_1} and ΔE_{B_2} can be related to the back-donations **8b,8c** from the two π^*_{CX} orbitals to b_1 and b_2 of $Ru(CO)_4$, respectively. We can, in fact, as is done in Table II where we give the breakdown of D(Ru–CX), combine ΔE_{B_1} and ΔE_{B_2} into one term, ΔE_{BD}, representing the total back-donation. A more detailed account of our decomposition method is given in Ref 28.

It follows from Table II that donation, ΔE_{A_1}, and back-donation, ΔE_{BD}, are of equal importance for the bond dissociation energy D(Ru–CX), and that both terms contribute to the increase in D(Ru–CX) along the series X = O, S, Se, and Te, with the largest increment in ΔE_{A_1} and ΔE_{BD} occuring between CO and CS.

It is possible to relate the variations in ΔE_{A_1} as well as ΔE_{BD} to the order of electronegativity, O >> S > Se > Te, among the chalcogen atoms or to the rise in energy of the ns and np orbitals (n = 2, 5) on the chalcogen elements from oxygen to tellurium, which amounts to the same thing, (Figure 2A). Obviously, the

(25) (a) Lichtenberger, D. L.; Fenske, R. F. *Inorg. Chem.* **1976**, *15*, 2015. (b) Saillard, J. Y.; Grandhean, D.; Caillet, P.; Le Beuze, A. *J. Organomet. Chem.* **1980**, *190*, 371.
(26) (a) Butler, I. S.; Garcia-Rodriguez, A.; Plowman, K. R.; Shaw, C. F., III. *Inorg. Chem.* **1976**, *15*, 260i. (b) Baaibich, I. M.; English, A. M.; Butler, I. S. *Organometallics* **1984**, *3*, 1786. (c) Andrews, M. A. *Inorg. Chem.* **1977**, *16*, 499.
(27) Huber, K. P.; Herzberg, G. In *Molecular Spectra and Molecular Structure*; Van Nostrand Reinhold: New York, 1979; Vol. 4.
(28) (a) Ziegler, T.; Rauk, A. *Inorg. Chem.* **1979**, *18*, 1558. (b) Ziegler, T.; Rauk, A. *Inorg. Chem.* **1979**, *18*, 1755.

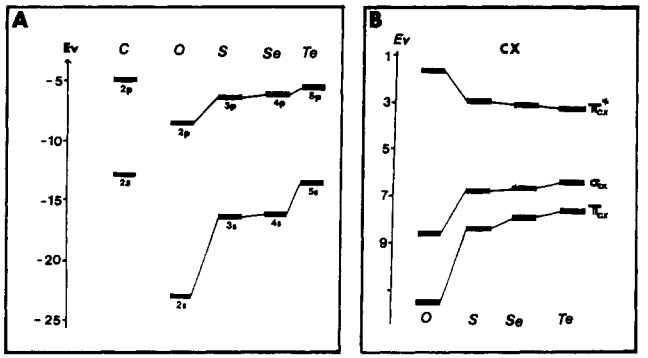

Figure 2. (A) Orbital energies (eVe for *n*s and *n*p of O, S, Se, and Te from HFS calculations. (B) Orbital energies (eV) for π_{CX}, σ_{CX}, and π^*_{CX} of CO, CS, CSe, and CTe from HFS calculations.

change in electronegativity will influence the orbital energies of σ_{CX}, π_{CX}, and π^*_{CX}, and any variation of the orbital energies will in turn reflect on the amount of donation and back-donation.

It is a simple matter to account for the trends in the energies of σ_{CX}, π_{CX}, and π^*_{CX} (Figure 2B) by using arguments[29] based on electronegativity perturbation. Thus, the π_{CX} orbital, which mainly is $2p_O$ in CO since $2p_O$ and $2p_C$ are far apart in energy (Figure 2A) will, as *n*p orbitals become similar in energy to $2p_C$ as *n* increases, have more participation from $2p_C$, and further be less bonding, since *n*p becomes more diffuse as *n* increases and is thus less able to overlap with $2p_C$. The energy of π_{CX} will on all three accounts, the reduced overlap as well as the rise in energy of *n*p and the increased participation from $2p_C$, rise in energy through the seriers CX = CO, CS, CSe, and CTe (see Figure 2B). The increase in energy and radial extent of *n*p as *n* increases will on the other hand cause π^*_{CX} to be less antibonding with more participation from *n*p and less from $2p_C$. The result is a decrease in energy of π_{CX}^* through the series X = O, S, Se, and Te on account of the reduced antibonding character and the increased participation from $2p_C$ (Figure 2B). The σ_{CX} orbital is only weakly bonding and consists on carbon of a sp-hybrid pointing away from X as well as a *n*p orbital on the chalcogen atom X. The energy of σ_{CX} is thus a sum of the energies of *n*p and the sp hybrid, and as *n*p rises in energy through higher values of *n*, so does σ_{CX} (Figure 2B).

The trends in the energies of σ_{CX}, π_{CX}, and π^*_{CX} (Figure 2B) can now, after their rationalization, be related to the calculated variations in ΔE_{A_1} and ΔE_{BD}. The decrease in energy of π_{CX}^* along the X = O, S, Se, and Te series will reduce the energy gap between b_1 and b_2 on $Ru(CO)_4$ and the two π^*_{CX} orbitals (Figure 3) and thus according to simple perturbational arguments[29] enhance ΔE_{BD}. The most pronounced drop in the energy of π^*_{CX}, as well as in the electronegativity of X, takes place between X = O and X = S (Figure 2) and causes here the most noticeable increment in ΔE_{BD} (Table II). The rise in energy of σ_{CX} in turn results in a smaller gap between $2a_1$ and σ_{CX} (Figure 3) and thus in a stronger donation interaction ΔE_{A_1} (Table II) through the series X = O, S, Se, and Te. We calculate the largest increment in ΔE_{A_1} to take place between CO and CS, where the changes in the energy of σ_{CX} and electronegativity of X are most pronounced.

A correlation between the energies of σ_{CX} and π^*_{CX} (Figure 2B) and the amount of charge donated or back-donated has previously been given by Lichtenberger and Fenske[25a] as well as Saillard et al.[25b] for CO, CS, and CSe.

The stretching frequency of coordinated CO is always observed to be reduced compared to that of the free ligand, and the few cases where it has been possible to carry out a force field analysis[26a] of a carbonyl complex have revealed that *k*(C–O) of complexed CO was smaller than *k*(C–O) of free CO; this is also what we calculate in the case of $Ru(CO)_5$ (Table I). The reduction in *ν*(C–O) and *k*(C–O) has been explained in terms of back-donation

(29) Albright, T. A.; Burdett, J. K.; Wangbo, M. H. *Orbital Interactions in Chemistry*; Wiley: New York, 1985.

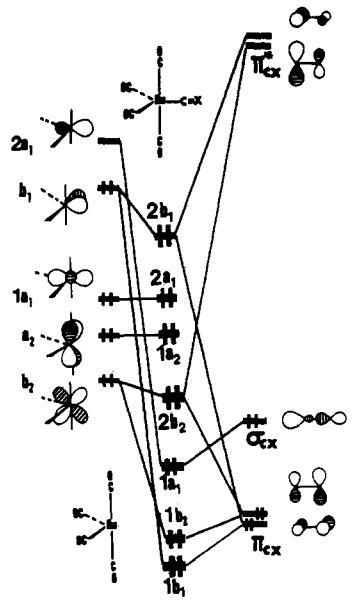

Figure 3. Interaction diagram between orbitals of $Ru(CO)_4$ (left) and CX (right) and the resulting orbital levels in $Ru(CO)_4CX$ (middle).

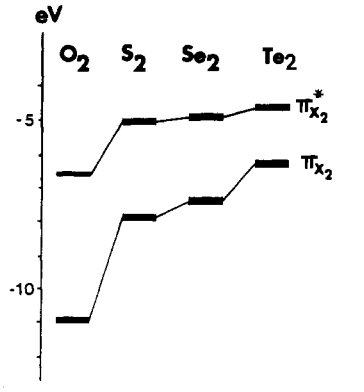

Figure 4. Orbital energies of π_{X_2} and $\pi^*_{X_2}$ for O_2, S_2, Se_2, and Te_2 in eV, from HFS calculations.

to the π^*_{CO} orbital and used extensively to probe the bonding in both substituted and unsubstituted carbonyl complexes.

The *ν*(C–S) stretching frequency of complexed CS has on the other hand been observed[26c] in the range 1106–1409 cm^{-1} at both higher and lower frequencies than *ν*(C–S) of free CS at 1279 cm^{-1}, and a force field analysis[26a] of $W(CO)_5CS$ has revealed *k*(C–S) at 8.2 mdyn $Å^{-1}$ to be very similar to *k*(C–S) of the free CS ligand at 8.4 mdyn $Å^{-1}$. In our calculations on $Ru(CO)_4CX$ we find *k*(C–X) to be close to the same value for complexed and free CX, not only the X = S but also for X = Se and Te.

It is perhaps surprising that the back-donation to π^*_{CX} in ML_nCX only reduces *k*(C–X) and *ν*(C–X) substantially and consistently for X = O, whereas some thiocarbonyl complexes in fact have a higher *ν*(C–X) stretching frequency than free CS, in view of the fact that back-donation to π^*_{CX} in general is assumed to increase through the series X = O, S, Se and Te, as in our calculations in $Ru(CO)_4CX$ where we find the total occupation of the two π^*_{CX} orbitals to be 0.45, 0.55, 0.61, and 0.65 for O, S, Se, and Te, respectively.

We can explain this apparent disparity by noting that the force constant *k*(C–X) for the C–X stretch can be written as

$$k(\text{C–X}) = 2(\Delta E)/(\Delta R)^2 \qquad (2)$$

where ΔE is the total energy required to elongate (or contract) the C–X bond from the equilibrium distance by ΔR. In free CX we have $\Delta E = \Delta E^\circ$, where the positive term ΔE° simply is the energy required to weaken the CX bond as it is stretched. In coordinated CX we have, on the other hand

$$\Delta E = \Delta E^\circ + \Delta E_\pi + \Delta E_\sigma. \qquad (3)$$

Table III. Optimized R(Ru-X) and R(X-X) Bond Distances (Å) as well as a Decomposition of Calculated $D(Ru-X_2)$ Bond Energies (kJ mol^{-1}) in $Ru(CO)_4X_2$ (X = O, S, Se, Te)

X_2	R(Ru-X)	R(X-X)	ΔE_{prep}	$\Delta E°$	ΔE_{A_1}	ΔE_{B_1}	$\Delta E_{A_2} + \Delta E_{B_2}$	$D(Ru-X_2)^a$
O_2	1.93	1.39 (1.21)[b]	−331	−243	102	594	11	133
S_2	2.23	2.08 (1.89)	−200	−143	117	443	27	244
Se_2	2.36	2.34 (2.17)	−177	−119	125	392	25	246
Te_2	2.47	2.78 (2.56)	−165	−48	134	296	23	240

[a] $D(Ru-X_2) = \Delta E_{prep} + \Delta E° + \Delta E_{A_1} + \Delta E_{A_2} + \Delta E_{B_1} + \Delta E_{B_2}$. [b] Experimental R(X-X) distance for free X_2.[27]

The last term in eq 3, ΔE_{π^*}, is negative and stems from a strengthening of the M–CX bond through increasing back-donation to π^*_{CX}, as the π^*_{CX} orbital is lowered in energy by stretching the C-X bond and is thus better able to interact with b_1 and b_2 of $Ru(CO)_4$ (Figure 3). The second term, ΔE_π, is positive, and stems from a weakening of the M–CX bond through increasing 4-electron destabilizing interactions between the occupied b_1 and b_2 metal orbitals and the two occupied π_{CO} orbitals, as π_{CX} rises in energy on stretching the CX bond (Figure 3). It can be seen by combining eq 3) and eq 2 that ΔE_{π^*} will reduce k(C–X) and ΔE_π will increase k(C–X). The first term in eq 3 is the remainder, representing the weakening of the C–X bond as the C–X distance is stretched without considering any change in back-donation. The term $\Delta E'°$ has thus the same meaning as $\Delta E°$ of free CX.

For CO where π_{CO} is low in energy (Figure 2B), the gap between b_1, b_2, and the two π_{CO} orbitals (Figure 3) is large, and ΔE_{π^*} will prevail over ΔE_π, leading to a reduction in k(C–O). In the case of CS, CSe, and CTe, where the energy of π_{CX}, for reasons given previously, is much higher than the energy of π_{CO} (Figure 3), both ΔE_{π^*} and ΔE_π will be of importance, and since they are of opposite signs, they largely cancel in (2) with the result that f(C–X) is nearly the same for complexed and free CX in the case of X = S, Se, and Te (Table II).

V. Donor and Acceptor Abilities of O_2, S_2, Se_2, and Te_2 in $Ru(CO)_4X_2$ (X = O, S, Se, Te)

The structurally characterized d^8 complexes with O_2,[30] S_2,[6] and Se_2[10] as ligands all have a distorted-octahedral geometry where the dichalcogen ligand is coordinated side-on as in the structure chosen for our $Ru(CO)_4X_2$ model system (**9**).

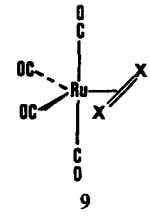

9

The X_2 molecule has in its ground state two singly occupied π^*-type orbitals, $\pi^*_{b_1}$ and $\pi^*_{a_2}$, of which $\pi^*_{b_1}$ is strongly interacting with the HOMO b_1 of $Ru(CO)_4$ in $Ru(CO)_4X_2$ (Figure 5) whereas $\pi^*_{a_2}$ is largely nonbonding, as well as two fully occupied π-type orbitals, π_{a_1} and π_{b_2}, of which π_{a_1} is strongly interacting with the LUMO of $Ru(CO)_4$ in $Ru(CO)_4X_2$, (Figure 5) whereas π_{b_2} mainly is nonbonding.

We have in order to delineate the importance of the interaction between $2a_1$ and π_{a_1}, in analogy with (1), decomposed the calculated bond energies $D(Ru-X_2)$, (Table III) into

$$D(Ru-X_2) = \Delta E_{prep} + \Delta E° + \Delta E_{A_1} + \Delta E_{B_1} + \Delta E_{B_2} \quad (4)$$

Here ΔE_{prep} has two contributions, one corresponding to the deformation of $Ru(CO)_4$ from **3** to **6** with $\theta = 100°$ (78 kJ mol^{-1}) and another representing the energy required to bring X_2 from its electronic ground-state configuration $^3\Sigma^+_g[(\pi^*_{b_1})^1(\pi^*_{a_2})^1]$ and equilibrium X–X distance, to the electronic configuration $[(\pi^*_{b_1})^0(\pi_{a_2})^2]$, where $\pi^*_{b_1}$ is completely vacated, at the R(X–X) distance of X_2 in $Ru(CO)_4X_2$. The additional terms in (3) have the same meaning as in (1), and ΔE_{B_1} thus represents the back-donation of charge from b_1 to the vacated $\pi^*_{b_1}$ orbital, wheras ΔE_{A_1} is related to the donation of charge from π_{a_1} to $2a_1$ (Figure 4). It follows from Table III, where we give $D(Ru-X_2)$ decomposed into the various components, that the back-donation, ΔE_{B_1}, is more important than the donation, ΔE_{A_1}u, for the calculated stabilities of the $Ru(CO)_4X_2$ adducts, in agreement with previous theoretical investigations on d^8 dioxygen complexes.[30]

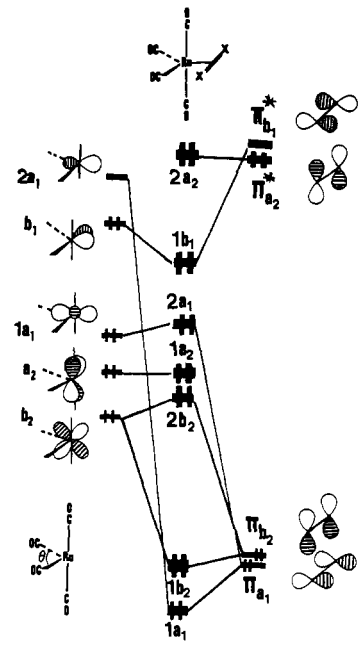

Figure 5. Interaction diagram between orbitals of $Ru(CO)_4$ (left) and X_2 (right) and the resulting orbital levels in $Ru(CO)_4X_2$ (middle).

The energies of $\pi^*_{b_1}$ and π_{a_1} increase through the series X = O, S, Se, and Te due to the rise in energy of np on the chalogen atoms for higher values of n, (see Figure 4). The contribution to $D(Ru-X_2)$ from the back-donation process, ΔE_{B_1}, will as a consequence decrease from O_2 to Te_2 as the energy gap between b_1 and $\pi^*_{b_1}$ becomes larger (Figure 4 and Figure 5), with the most substantial change between X = O and X = S (Table III), whereas the contribution to $D(Ru-X_2)$ from the donation process, ΔE_{A_1}, increases through the series X = O, S, Se, and Te as the energy gap between $2a_1$ and π_{b_1} becomes smaller (Figure 4 and Figure 5), again with the most pronounced change between X = O and X = S (Table III). We find from population analyses in line with the calculated trends of ΔE_{A_1} and ΔE_{B_1}, that 1.04e, 0.91e, 0.89e, and 0.78e are back-donated from b_1 to $\pi^*_{b_1}$ for O, S, Se, and Te, respectively, with 0.24e, 0.43e, 0.51e, and 0.65e donated from π_{a_1} to $2a_1$ for O, S, Se, and Te, respectively.

Considering only the electronic terms ΔE_{A_1}, ΔE_{B_1}, and $\Delta E_{A_2} + \Delta E_{B_2}$, one would conclude (Table III) that the dioxygen adduct should be more stable than the thio, seleno, and telluro analogues. When, however, the electronic terms are combined with $\Delta E°$ and ΔE_{prep} into $D(Ru-X_2)$, one finds in fact the dioxygen complex to have the smallest calculated bonding energy $D(Ru-O_2)$ (Table III) and to be less stable than the other dichalcogen adducts due to $\Delta E°$ and ΔE_{prep}. The negative and destabilizing steric term $\Delta E°$, representing the 4-electron destabilizing interactions between occupied orbitals on $Ru(CO)_4$ and X_2, is most pronounced for $Ru(CO)_4O_2$ with relatively short Ru–O distances, and the negative term ΔE_{prep} is likewise most important for $Ru(CO)_4O_2$ as more

(30) (a) Norman, J. G.; Ryan, P. B. *Inorg. Chem.* **1982**, *21*, 3555. (b) Vaska, L. *Acc. Chem. Res.* **1968**, *1*, 335. (c) Vaska, L. *Acc. Chem. Res.* **1976**, *9*, 175.

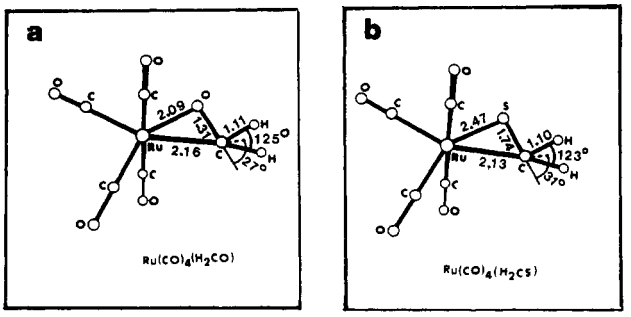

Figure 6. (A) Optimized coordination geometry of H_2CO in $Ru(CO)_4(\eta^2\text{-}H_2CO)$ (distances in Å). (B) Optimized coordination geometry of H_2CS in $Ru(CO)_4(\eta^2\text{-}H_2CS)$ (distances in Å).

energy is required to promote X_2 from the electronic ground-state configuration $^3\Sigma^+_g[(\pi^*_{b_1})^1(\pi^*_{a_2})]$ to $[(\pi_{b_1})^0(\pi_{a_2})^2]$ for X = O than for X = S, Se, and Te (Table III). Bonding energies are not known for $Ru(CO)_4X_2$ or analogous systems, but Clark et al.[31] have, in agreement with the calculated trends for $D(Ru\text{–}X_2)$, observed that d^8 complexes coordinate S_2 and Se_2 more readily than O_2.

The bond orders for the complexed dichalcogens in $Ru(CO)_4X_2$ have compared to that of free X_2, by a little more than 1, on account of the donation as well as the back-donation, and it is thus not surprising that the optimized $R(X\text{–}X)$ distances in $Ru(CO)_4X_2$ are longer, by 0.2 Å, than $R(X\text{–}X)$ of free X_2 (Table III). In fact, the optimized $R(X\text{–}X)$ distances in $Ru(CO)_4X_2$ are for X = O and S quite similar to the interatomic distances in O_2^- and S_2^-, respectively, and furthermore compare well with $R(X\text{–}X)$ values determined by X-ray diffraction measurements on d^8 complexes of O_2,[30] S_2,[6] and Se_2.[10]

VI. Donor and Acceptor Abilities of H_2CO, H_2CS, CO_2, and CS_2 in Complexes with $Ru(CO)_4$

Formaldehyde and carbon dioxide, as well as their thio, seleno, and telluro analogues, all have occupied π orbitals and vacant π^* orbitals suitable for side-on coordination of the form indicated in **10a, b**. To date only a few formaldehyde[4] or thioformaldehyde[8]

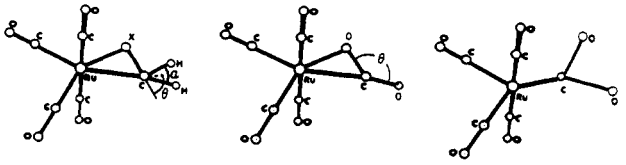

10a **10b** **10c**

complexes have been structurally characterized, all with the side-on geometry of **10a**. The coordination chemistry of carbon dioxide[3] and carbon disulfide[7] has, on the other hand, proven to be rather versatile, with CX_2 bound through carbon (**10c**) or one of the X atoms as well as side-on bound via the η^2-C=X functionality (**10b**).

It is apparent from our analysis of the bonding in $Ru(CO)_4CX$ and $Ru(CO)_4X_2$ that the variation in the $D(Ru\text{-}CX)$ and $D(Ru\text{-}X_2)$ bond energies along the X = O, S, Se, and Te series is most notable between oxygen and sulfur, where we have the most substantial jump in electronegativity. We shall thus, in our comparison of oxo ligands with their chalco analogues, in the cases of H_2CX and CX_2, restrict the comparison to that between H_2CO and CO_2 and the thio analogues H_2CS and CS_2.

We give in Figure 6 the optimized structures of $Ru(CO)_4(H_2CO)$ and $Ru(CO)_4(H_2CS)$. Most noticeable is a distortion from planarity of the H_2CX ligand, with the X–CH_2 dihedral angle for complexed H_2CX optimized at $\theta = 27°$ (X = O) and $\theta = 31°$ (X = S), respectively, as well as an elongation of the C–X bond compared to that in free H_2CX, from 1.61 to 1.74 Å in the case of H_2CS and from 1.20 to 1.31 Å in the case of H_2CO. The two distortions will raise the energy of π_{H_2CX} and lower the energy of $\pi^*_{H_2CX}$, and thus in both cases serve to enhance the donation (**11a**) as well as the back-donation (**11b**). The distortion from

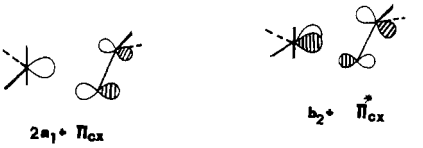

11a **11b**

planarity will further optimize the directionality of the p-lobe on carbon in the back-bonding interaction **11b**. The optimized C–O bond length (1.31 Å) of $Ru(CO)_4(H_2CO)$ (see Figure 6) is very close to those observed[4] for formaldehyde complexes (~1.35 Å), with the exception[4c] of $Os(CO)_2(PPh_3)_2(\eta^2\text{-}CH_2O)$, where $R(CO)$ = 1.59 Å. It has not been possible experimentally to locate the hydrogen atoms in formaldehyde complexes; we expect the optimized dihedral angles θ to be reasonable estimates.

In decomposing the bonding energies of $Ru(CO)_4CX$ and $Ru(CO)_{X2}$, respectively, use was made of the fact that donation and back-donation involved orbitals of different symmetries. The low C_S point-group symmetry of $Ru(CO)_4(H_2CX)$ does not allow for a symmetry separation of **11a** and **11b**; in fact both interactions involve orbitals in the a′ representation, and we can thus not use our standard decomposition scheme. We can, however, make use of a similar decomposition scheme due to Kitaura and Morokuma.[32] The bonding energy $D(Ru\text{–}CH_2X)$ can, in this scheme, be written as

$$D(Ru\text{–}CH_2X) = \Delta E_{prep} = \Delta E° + \Delta E_D + \Delta E_{BD} + \Delta E_{mix} \quad (5)$$

where $\Delta E°$ is the steric interaction energy and ΔE_D and ΔE_{BD} are the contributions to $D(Ru\text{–}CH_2X)$ from **11a** and **11b**, respectively, whereas ΔE_{prep} represents the energy required to deform H_2CX from planarity and $Ru(CO)_4$ from $\theta = 120°$ to $\theta = 100°$. The term ΔE_{mix} represents the coupling between **11a** and **11b** due to the fact that the two processes take place in the same symmetry representation.

Table IV. Decomposition of Calculated Bond Energies ΔE (kJ mol^{-1}) for Bonds between $Ru(CO)_4$ and the Ligands H_2CX and CX_2 (X = O, S)

ligand	ΔE_{prep}	$\Delta E°$	ΔE_D	ΔE_{BD}	ΔE_{mix}	ΔE
H_2CO	−169.9	−155.2	123.7	345.6	37.1	181.3[a]
H_2CS	−158.2	−163.8	159.1	359.3	31.5	227.9
CO_2	−186.3	−141.2	118.9	271.0	39.9	102.3
CS_2	−201.5	−128.1	132.4	318.3	36.8	157.9

[a] $\Delta E = \Delta E_{prep} + \Delta E° + \Delta E_D + \Delta E_{BD} + \Delta E_{mix}$.

It follows from Table IV, where we give the bonding energies $D(Ru\text{–}H_2CX)$ (X = O, S) decomposed into the various components, that the back-donation ΔE_{BD} in terms of energy is more important for the stability of $Ru(CO)_4(H_2CS)$ than the donation ΔE_D. In terms of charge, 0.30e (X = O) and 0.46e (X = S) were donated (**11a**) from π_{H_2CX} to the LUMO of $Ru(CO)_4$ and 0.74e (X = O) and 0.76 (X = S) back-donated (**11b**) from the HOMO of $Ru(CO)_4$ to $\pi^*_{H_2CX}$. Thioformaldehyde is calculated to be more strongly bound to $Ru(CO)_4$ than formaldehyde (Table IV) as a result of more favorable contributions from ΔE_{BD} and in particular ΔE_D. The contribution for ΔE_D is larger for X = S than for X = O because π_{H_2CS}, for reasons similar to those used to rationalize the relative energies of π_{CX}, is higher in energy (by 1 eV.) than π_{H_2CO} and thus is better able to interact with the LUMO of $Ru(CO)_4$. The overlaps between the LUMO of $Ru(CO)_4$ and π_{H_2CX} are 0.29 (X = S) and 0.26 (X = O), respectively, and thus more favorable in the first case. We note in connection with the back-donation ΔE_{BD}, that π_{H_2CS} is lower in energy (by 0.3 eV.) than π_{H_2CO}, and overlaps better with the HOMO of $Ru(CO)_4$ than $\pi^*_{H_2CO}$, 0.27 (X = S) as compared to 0.23 (X = O).

We have considered conformation **10b** as well as **10c** for CX_2 complexed to $Ru(CO)_4$ and found **10b** to be more stable than **10c** by 145 (X = O) and 126 kJ mol^{-1} (X = S), respectively. The

(31) Clark, G. R.; Russell, D. R.; Roper, W. R.; Walker, A. *J. Organomet. Chem.* **1977**, *136*, C1.

(32) Sakaki, S.; Kitaura, K.; Morokuma, K. *Inorg. Chem.* **1982**, *21*, 760.

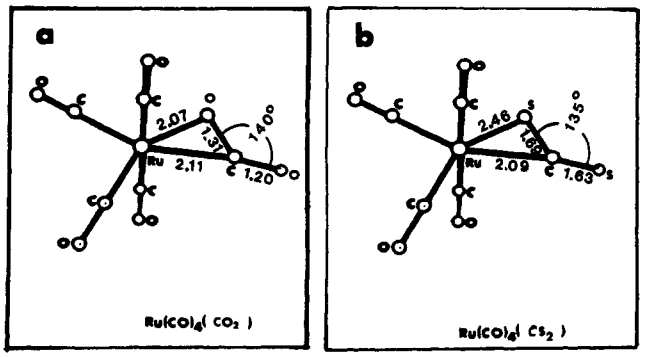

Figure 7. (A) Optimized coordination geometry of CO_2 in $Ru(CO)_4$-(η^2-CO_2) (distances in Å). (B) Optimized coordination geometry of CS_2 in $Ru(CO)_4(\eta^2$-$CS_2)$ (distances in Å).

optimized structures of $Ru(CO)_4CX_2$ in conformation **10b** are given in Figure 7. Complexed carbon dioxide and carbon disulfide are not linear, but bent from $\theta = 180°$ to $\theta = 145°$ (X = O) and $\theta = 135°$ (X = S), respectively. The C–X distance in the η^2-C=X functionality is further elongated from 1.20 (free CO_2) to 1.33 Å for CO_2 and from 1.65 (free CS_2) to 1.71 Å in the case of CS_2. Both deformations are in line with those observed[3,7] in experimental structure determinations of CX_2 complexes and serve as already explained by Sakaki et al.[32] to lower the energy of π_{CX_2} and raise the energy of $\pi^*_{CX_2}$ so as to enhance both the donation (**12a**) and the back-donation (**12b**).

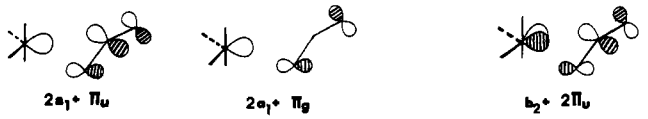

12a **12b**

The CS_2 ligand is seen from Table IV to be more strongly bound to $Ru(CO)_4$ than CO_2. An analysis revealed that this is so for much the same reason that H_2CS is more strongly bound to $Ru(CO)_4$ than H_2CO, namely the lower energy of $\pi^*_{CS_2}$ and higher energy of π_{CS}, as well as better overlaps of π_{CS_2} and $\pi^*_{CS_2}$ with the LUMO and HOMO of $Ru(CO)_4$, respectively, in comparison with the corresponding π_{CO_2} and $\pi^*_{CO_2}$ orbitals. Back-donation, ΔE_{BD}, is seen, (Table IV) to be more important than donation, ΔE_D, for the stability of $Ru(CO)_4CX_2$, and we calculate 0.62e (X = O) and 0.83e (X = S), respectively, to be back-donated to $\pi^*_{CX_2}$ from the HOMO of $Ru(CO)_4$, with 0.30e (X = O) and 0.39e (X = S), respectively, donated from π_{CX_2} to the LUMO of $Ru(CO)_4$.

It follows from Table IV that H_2CX is more strongly bound to $Ru(CO)_4$ than CX_2 in the case of the oxo ligands as well as their thio analogues. The determining factor for this trend is, according to our analysis, that π_{CX_2} and $\pi^*_{CX_2}$ have smaller overlaps with the metal orbitals (**12**) than π_{H_2CX} and $\pi^*_{H_2CX}$ (**11**). This is primarily so because π_{CX_2} and $\pi^*_{CX_2}$ are delocalized over three atoms but only interact through two (**12**), whereas π_{H_2CX} and $\pi^*_{H_2CX}$ only are delocalized over the two atoms through which they are interacting (**11**).

VII. Concluding Remarks

We have presented calculated coordination geometries and bond energies for CX and X_2 (X = O, S, Se, Te) as well as H_2CX and CX_2 (X = O, S) complexes with $Ru(CO)_4$. We find that the bond energies increase strongly from complexes of the oxo ligands CO, O_2, H_2CO, and CO_2 to complexes of the analogous thio ligands CS, S_2, H_2CS, and CS_2, whereas the change (increase) in bond energy from complexes of the thio ligands to complexes of their seleno and telluro analogues is much smaller. The trends have been related to a drastic drop in electronegativity between oxygen and sulfur followed by a modest decrease from sulfur to tellurium in the cases of CX, H_2CS, and CX_2. The drop in electronegativity from oxygen to tellurium will, in fact, for the dichalcogen adducts $Ru(CO)_4X_2$ cause the interaction between O_2 in its valence singlet state and $Ru(CO)_4$ to be larger than the corresponding interactions between $Ru(CO)_4$ and the other singlet dichalcogen X_2 (X = S, Se, Te). However, the energy required to promote X_2 from its triplet ground state to the singlet valence state is considerably larger for X = O than for X = S, Se, and Te. The overall adduct formation energy between $Ru(CO)_4$ and O_2 is as a consequence smaller than the adduct formation energies between $Ru(CO)_4$ and the other dichalcogens X_2 (X = S, Se, Te).

HFS calculations have, in the past,[13,14,28] reproduced geometrical parameters rather well, and we expect the optimized bond distances presented here to be correct to within ±0.03 Å, with an error bound of ±5° for the optimized bond angles. The HFS method tends, on the other hand, to overestimate[33b] bond energies for systems of the type discussed here. The bond energies might thus, in absolute terms, have an error of as much as 40 kJ mol^{-1}. We feel, however, that relative energies are correctly represented. Work is currently in progress[33] to remedy some of the shortcomings of the HFS method.

Acknowledgment. This investigation was supported by the Natural Sciences and Engineering Research Council of Canada (NSERC). We thank Professor E. J. Baerends (The Free University of Amsterdam) for providing us with the newest version of the HFS program system, and Mr. P. Vernooijs (The Free University of Amsterdam) for installing the HFS programs at the Cyber-205 installation at the University of Calgary.

Registry No. **1**, 102630-34-2; **7** (X = S), 102648-61-3; **7** (X = Se), 102648-62-4; **7** (X = Te), 102648-63-5; **9** (X = O), 102630-35-3; **9** (X = S), 102630-36-4; **9** (X = Se), 102630-37-5; **9** (X = Te), 102630-38-6; $Ru(CO)_4H_2CO$, 102630-39-7; $Ru(CO)_4H_2CS$, 102630-40-0; $Ru(CO)_4$-CO_2, 102630-41-1; $Ru(CO)_4CS_2$, 102630-42-2.

(33) (a) Becke, A. submitted for publication in *J. Chem. Phys.* (b) Tschinke, V.; Ziegler, T. Presented at the International Conference on Quantum Chemistry, Montreal, 1985. Calculations on the first CO dissociation energy of $Ni(CO)_4$, $Fe(CO)_5$, $Mo(CO)_6$, and $W(CO)_6$ were performed by the HFS method as well as the density functional suggested by Becke in ref 33a.

(34) The periodic group notation in parentheses is in accord with recent actions by IUPAC and ACS nomenclature committees. A and B notation is eliminated because of wide confusion. Groups IA and IIA become groups 1 and 2. The d-transition elements comprise groups 3 through 12, and the p-block elements comprise groups 13 through 18. (Note that the former Raman number designation is preserved in the last digit of the new numbering: e.g., III → 3 and 13.)